

Short communication

Developments of new proton conducting membranes based on different polybenzimidazole structures for fuel cells applications

A. Carollo^a, E. Quartarone^{a,*}, C. Tomasi^a, P. Mustarelli^a, F. Belotti^a, A. Magistris^a,
F. Maestroni^b, M. Parachini^b, L. Garlaschelli^b, P.P. Righetti^b

^a Department of Physical Chemistry, IENI-CNR and INSTM, University of Pavia Via Taramelli 16, 27100 Pavia, Italy

^b Department of Organic Chemistry, University of Pavia Via Taramelli 12, 27100 Pavia, Italy

Received 13 December 2005; received in revised form 25 January 2006; accepted 27 January 2006

Available online 23 March 2006

Abstract

The current goal on PEMFCs research points towards the optimization of devices working at temperatures above 100 °C and at low humidity levels. Acid-doped polybenzimidazoles are particularly appealing because of high proton conductivity without humidification and promising fuel cells performances.

In this paper we present the development of new proton conducting membranes based on different polybenzimidazole (PBI) structures. Phosphoric acid-doped membranes, synthesized from benzimidazole-based monomers with increased basicity and molecular weight, are presented and discussed. Test of methanol crossover and diffusion were performed in order to check the membrane suitability for DMFCs.

Both the acid doping level and proton conductivity remarkably increase with the membrane molecular weight and basicity, which strictly depend on the amount of NH-groups as well as on their position in the polymer backbone. In particular, a conductivity value exceeding 0.1 S cm⁻¹ at RH = 40% and 80 °C was reached in the case of the pyridine-based PBI.

© 2006 Elsevier B.V. All rights reserved.

Keywords: Fuel cells; Proton exchange membranes; Polybenzimidazole (PBI); Phosphoric acid

1. Introduction

The current research on PEMFCs is focused on the optimization of a device working at operational temperatures above 100 °C and at very low humidity levels [1]. Such operative conditions offer several advantages [1], such as an enhanced catalyst stability towards the fuel impurities, a faster electrode kinetics and chiefly a simplified water management design, which is particularly important in the case of stationary applications.

The optimization of high-temperature PEMFCs requires the development of new membranes in which the proton transport is not assisted by the water molecules. In the case of Nafion, whose proton conductivity is acceptable only at elevated hydration levels, this peculiar limit was partially solved by preparing composite membranes with active nanofillers [2,3]. In particular,

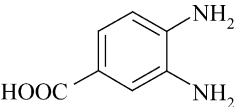
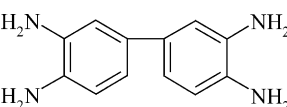
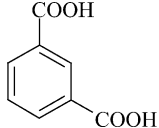
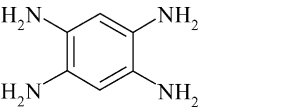
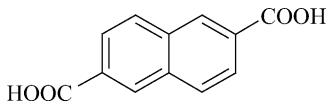
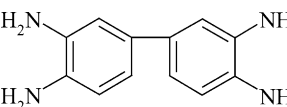
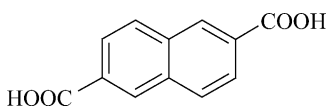
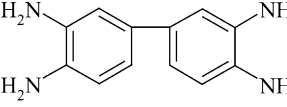
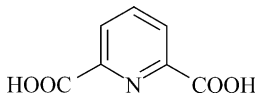
quite promising systems are based on composites of Nafion and insoluble three-dimensional zirconium phosphates with high proton conductivity even at relative humidity less than 1% [3].

In order to extend the temperature range, the attention was focused on membranes with thermal stability higher than Nafion itself. Several recent reviews well depict the state of the art on new polymers suitable as electrolytes for fuel cells. Many alternatives were proposed to this aim, ranging on a wide group of ionomers, like modified perfluoropolymers, ormolytes, blends of acid and base aromatic polymers [4–7].

Acid-doped polybenzimidazoles [8] are particularly appealing because of high proton conductivity with no or low humidification and promising fuel cells performances [9]. PBI, in fact, contains basic functional groups which can easily interact with strong acids, such as H₃PO₄ and H₂SO₄, so allowing proton migration along the anionic chains via Grotthuss mechanism [10,11]. In particular, poly-(2,2'-*m*-phenylene-5,5'-bibenzimidazole) was widely investigated for what concerns synthetic approach and casting process [9], membrane ther-

* Corresponding author. Tel.: +39 0382 987894; fax: +39 0382 987895.
E-mail address: elena.quartarone@unipv.it (E. Quartarone).

Table 1
PBI-based polymers: condensation monomers and acid doping level of the corresponding membranes, expressed as N' = mol (H_3PO_4)/mol (polymer unit)

Polymer	Monomer A	Monomer B	N'
ABPBI		–	1.1
PBI.4N			4.5
PBI.4N.a			6.1
PBI.4N.b			10.4
PBI.5N			12.0

ABPBI: poly(2,5-benzimidazole); PBI.4N: poly(2,2'-(*m*-phenylene)-5,5'-bibenzimidazole); PBI.4N.a: poly(2,6-(2,6-naphthylidene)-1,7-dihydrobenzo[1,2-*d*;4,5-*d'*]diimidazole); PBI.4N.b: poly(2,2'-(2,6-naphthylidene)-5,5'-bibenzimidazole); PBI.5N: poly(2,2'-(2,6-pyridin)-5,5'-bibenzimidazole).

mal stability [12], methanol crossover [7], acid doping procedure, proton transport [10,11,13,14], and fuel cells performances [7,15–19]. High-temperature, PBI-based MEAs (Celtec®) for PEMFCs were developed by Celanese [20].

Anyway, the proton conductivity of the doped PBI membranes exceeds 0.05 S cm^{-1} only above 150°C [7,9], which is actually above the expected operative range of both automotive and stationary applications. In order to increase the proton conductivity at lower temperatures, the membrane acid doping needs to be enhanced, but this worsens the membrane mechanical properties. Several ways have been proposed in order to overcome this limit, including addition of inorganic fillers [21] or heteropolyacids [22–24], sulfonation of the polybenzimidazole [25,26], or even preparation of porous films to be soaked in concentrated acid solutions [27]. Recently, a new synthetic approach has been reported, that carries out in situ doping during the casting process which is performed directly from the polymerization solution [28]. However, in spite of this large amount of information, only few and isolated efforts to change the basic monomer structure of PBI have been reported [29–32].

In this paper we present the development of new proton conducting membranes based on different polybenzimidazole structures for fuel cells applications. Phosphoric acid-doped membranes, synthesized from BI-based monomers with increased basicity and molecular weight are presented and characterized. The membranes thermal stability, acid doping and proton conductivity are compared with those of poly(2,5-benzimidazole) (ABPBI) and poly-phenylene-benzimidazole (PBI.4N) and dis-

cussed in terms of the number and interspacing of the NH-groups in the monomer unit.

2. Experimental

2.1. The PBI-based polymers

All the synthesized PBI polymers are reported and labelled in Table 1. The polymer powders were prepared via a monomer condensation process, following the approach suggested by Asensio and Gomez-Romero [29]. In each case, the monomers were dissolved in polyphosphoric acid (PPA, 85% P_2O_5) and polymerized at 200°C under nitrogen atmosphere for 5 h (ABPBI) and 30 h (all the other systems). After the condensation reaction, the polymers were soaked in distilled water, in order to eliminate any residual of monomer and PPA, and subsequently treated with a NaOH solution (10 wt%). The polymers were then washed in boiling water, and finally dried under vacuum for 24 h.

2.2. The membrane casting and the acid doping

Films with thickness of $\sim 80 \mu\text{m}$ were prepared by casting a polymer solution of methanesulfonic acid onto a Petri dish and by evaporating the solvent at 160°C under a ventilated hood. The films were then boiled in distilled water for 1 h, dried and finally soaked into a H_3PO_4 solution (75 wt%) for 72 h. After the acid activation, each sample was dried under vacuum at 100°C for 24 h. The absorbed amount of H_3PO_4 was detected

by weighing the membranes before impregnation and after drying. The doping level, N' , expressed as the number of H_3PO_4 molecules per monomer unit, is reported in Table 1 for each membrane.

2.3. Characterization

The DSC measurements were performed with a 2910 MDSC (TA Instruments) by using silver pans, at a rate of $5^\circ C \text{ min}^{-1}$ under nitrogen purge. TGA scans were also recorded at $5^\circ C \text{ min}^{-1}$ under nitrogen flow with a 2950 TGA (TA Instruments). In order to investigate the thermal stability of the samples under conditions similar to the operating ones, we also have performed isothermal TGA experiments at $80^\circ C$ and 40% RH.

The proton conductivity was measured by means of the impedance spectroscopy technique, using a frequency response analyser (FRA Solartron 1255), connected to an electrochemical interface (Solartron 1287), over the frequency range 1 Hz–1 MHz, by applying a voltage of 100 mV. The membrane was fixed to a four-point measure cell put in a homemade climatic chamber. The check of the operating conditions (sample temperature and relative humidity) was performed by means of a thermo-hygroscopic probe (Rotronic). The impedance scans were performed with the following protocols: (i) at $80^\circ C$ ranging from 0 to 40% RH; (ii) by increasing the temperature from room temperature to $130^\circ C$ at the constant moisture level of 40% RH. The films were allowed to equilibrate 3–4 h at each moisture level before of the measurements.

The methanol permeability through the membranes was determined at $25^\circ C$ by using a standard split cell. The membranes (surface area of 4.9 cm^2) were vertically placed between two sections of identical volume (37 cm^3) containing a 2 M methanol solution and deionized water, respectively. The solutions were magnetically stirred so that methanol could reach the equilibrium on both chambers. Aliquots of $1 \mu\text{l}$ were taken at different times in the water reservoir, and the methanol concentration was measured by means of a gas chromatograph equipped with a flame ionization detector (Perkin-Elmer, Clarus 500).

X-ray powder diffraction (XRPD) patterns were collected on all of the samples using a Bruker-D8 Advance Diffractometer, employing Cu anticathode radiation. Measurements were performed in the 2θ range from 5° to 50° with a scan step of 0.02° and a fixed counting time of 5 s for each step.

A Canon-Fenske capillary viscosimeter was used in order to measure the intrinsic viscosity $[\eta]$ at $20^\circ C$, of (0.2–0.5%) polymer solutions in H_2SO_4 96–98%.

3. Results and discussion

3.1. The polymers intrinsic viscosity

Table 2 reports the intrinsic viscosity for each synthesized polymer, calculated by means of the following relationship:

$$[\eta] = K' DP^a$$

where K' and a are the Mark-Houwink constants and DP is the degree of polymerization, which is related to the polymer molecular weight through the relationship $DP = MW_{\text{pol}}/MW_{\text{mon}}$. The Mark-Houwink constants of ABPBI are 8.7^{-3} and 1.10, respectively [29], and we used these values even for the other investigated polymers whose constants, to our knowledge, are not reported in the literature. Therefore, in these last cases the intrinsic viscosity can only provide a rough estimate of the polymer molecular weight.

The detected ABPBI viscosity is in fair agreement with what measured by Asensio and Gomez-Romero under similar synthesis conditions [29]. However, higher viscosities, and consequently higher molecular weight, may be obtained by purifying the reaction monomers before the polymerization [29,31]. From the analysis of the parameters reported in Table 2, we can stress the following points: (i) the increase of the monomer molecular weight reduces the condensation rate; (ii) the enhanced basicity, provided by the presence of an extra N-atom in the PBI backbone (for example in the case of PBI_5N), determines an increase of the DP for equal condensation times, probably because of an improved monomer solubility in PPA. In any case, the obtained viscosity values are high enough to prepare films with satisfying handiness and processability.

3.2. The membranes thermal stability

Fig. 1 reports the TGA (part A) and DSC traces (part B), respectively, recorded on the doped membranes with $N' = 6.1$, 10.4 and 12.0. In each TGA curve one can observe an initial weight loss likely related to the release of surface adsorbed water, followed by a continuous mass decreases due to the condensation of PO_4 units. These weight losses are in agreement with what reported by Savinell and co-workers, which have deeply investigated the thermal rearrangement of phosphoric acid in doped-PBI membranes by means of TG-MS measurements [12]. Such evidences can be further corroborated by the DSC traces, where the endothermic peak occurring before $100^\circ C$ is certainly due to the loss of free water, whereas the following broad

Table 2
Intrinsic viscosity, $[\eta]$, polymerization degree, DP, and molecular weight, MW_{pol} , of the investigated PBI-based polymers

Membrane	$[\eta]$ (dl g^{-1})	DP	MW_{pol} ($g \text{ mol}^{-1}$)	MW_{mon} ($g \text{ mol}^{-1}$)	Casting process
ABPBI	3.36	225	26100	116	Mechanically strong film
PBI_4N	0.54	43	13244	308	Mechanically strong film
PBI_4N_a	0.41	34	9588	282	Mechanically strong film
PBI_4N_b	0.32	27	9666	358	Mechanically strong film
PBI_5N	0.68	53	16377	309	Mechanically strong film

MW_{mon} is the molecular weight of the corresponding monomer unit.

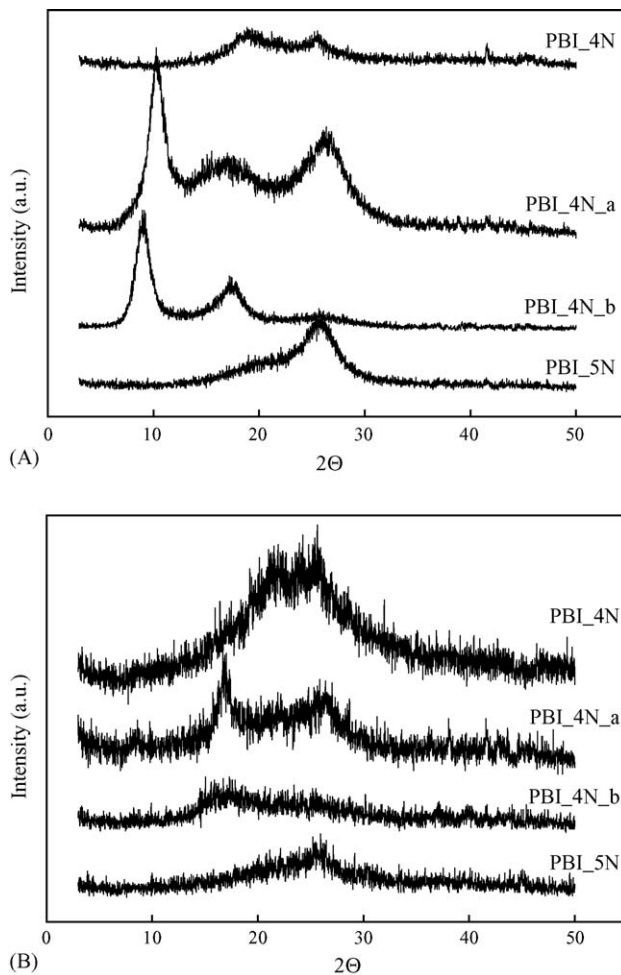
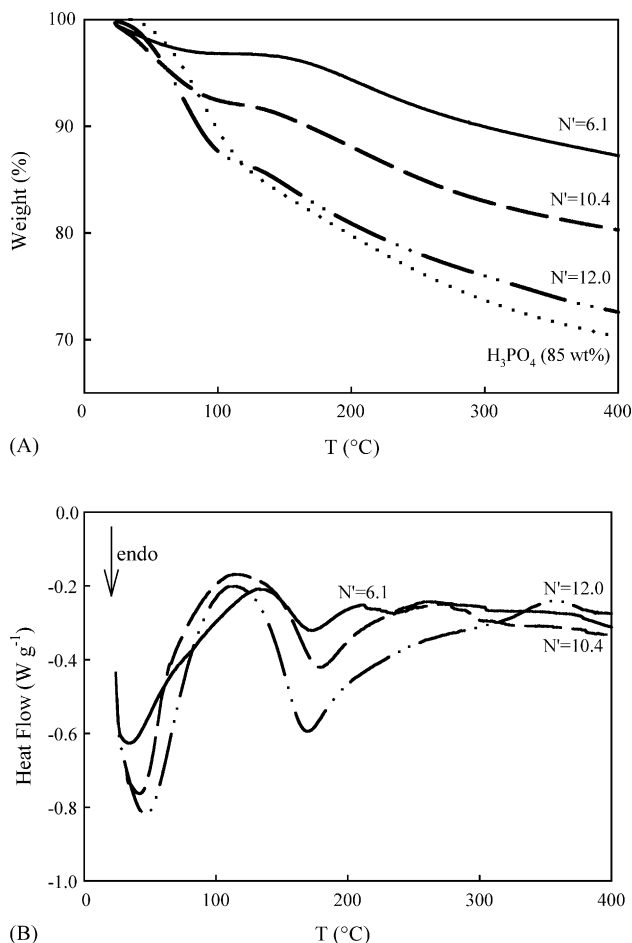


Fig. 1. (A) TGA curves of the PBI-based membranes, doped with H_3PO_4 : PBI_4N_a, $N' = 6.1$ (solid line); PBI_4N_b, $N' = 10.4$ (dashed line); PBI_5N, $N' = 12.0$ (dash-dot line); H_3PO_4 solution, 85% (dotted line). (B) DSC traces of the PBI-based membranes, doped with H_3PO_4 : PBI_4N_a, $N' = 6.1$ (solid line); PBI_4N_b, $N' = 10.4$ (dashed line); PBI_5N, $N' = 12.0$ (dash-dot line).

Fig. 2. XRD patterns of the undoped (A) and doped (B) PBI-based films.

endothermic feature accounts for the progressive elimination of H_2O molecules during the formation of polyphosphoric acid. As expected, the intensity of these phenomena increases by increasing the doping.

3.3. The membranes structural aspects

Fig. 2 compares the X rays diffraction patterns of the cast undoped (part A) and doped (part B) membranes based on PBI_4N, PBI_4N_a, PBI_4N_b and PBI_5N polymers. All the undoped films are semi-crystalline with a large amorphous fraction. In the case of PBI_4N_a three wide diffraction peaks are observed around 9° , 18° and 25° , which are assigned to the (100), (200) and (110) planes of poly-phenylenebenzimidazole [33], respectively. In particular, the peak at 25° is referred to the parallel orientation of the benzimidazole rings with respect to the film surface [34].

When the membranes are doped with the acid, the residual crystalline order is completely destroyed. The films are more amorphous for higher dopant content. On the other hand, phosphoric acid plays a plasticizing effect, as demonstrated by

remarkable T_g decreases observed by Hughes et al. in the DSC traces of the doped membrane [11]. The structure of PBI/ H_3PO_4 complexes was recently investigated and modelled [35].

3.4. The methanol permeability

The methanol permeation across a membrane is generally determined assuming molecular diffusion as predicted by Fick's law. As already described in Section 2, this measurement was performed by using a cell where the membrane is placed between two reservoirs containing methanol with constant concentration and water, respectively. The methanol concentration changes, c_B , in the pure water reservoir are related to the methanol diffusion, D , by the following linear relationship:

$$c_B(t) = \frac{A}{V_B L} DK c_A (t - t_0) \quad (2)$$

here A and L are the membrane area and thickness, respectively, V_B the water chamber volume, c_A the initial methanol concentration and t_0 is the so-called "time lag" which is related to the membrane permeability, $P = DK$, and K is the methanol partition coefficient. The permeation rate, or permeability, and t_0 are extracted from the linear regression of Eq. (2).

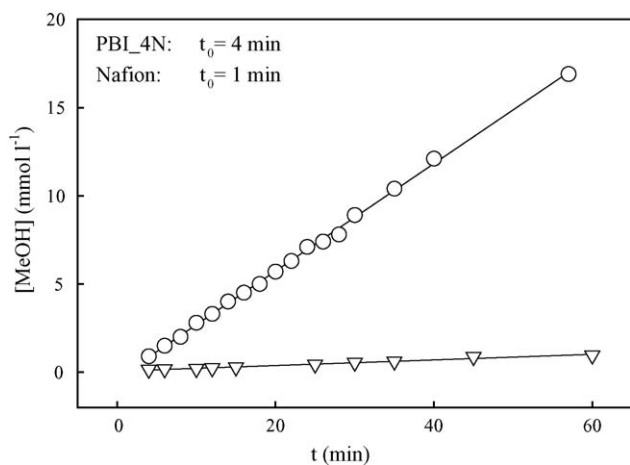


Fig. 3. Methanol concentration as a function of time at room temperature in the case of the PBI₄N membrane (open triangle) and of Nafion 117 (open circle). The lines are linear best-fits.

Fig. 3 compares the behaviour of the methanol concentration with time in the case of PBI₄N and NafionTM 117. In both the membranes the amount of MeOH diffused through the membrane changes linearly with the time. As expected, the methanol crossover through the PBI₄N film is remarkably lower than in the case of Nafion. The permeability values of the compared membranes are, in fact, 2×10^{-8} for PBI₄N and 1.0×10^{-6} cm² s⁻¹ for Nafion. Even lower P values were previously reported for polybenzimidazole membranes [36]. A PBI time lag four times longer than that of Nafion was finally determined (see Fig. 3).

3.5. The proton conductivity

Fig. 4 shows the proton conductivity values at 80 °C of all the investigated samples versus the relative humidity, RH. The data of Nafion 117 are reported for the sake of comparison. The

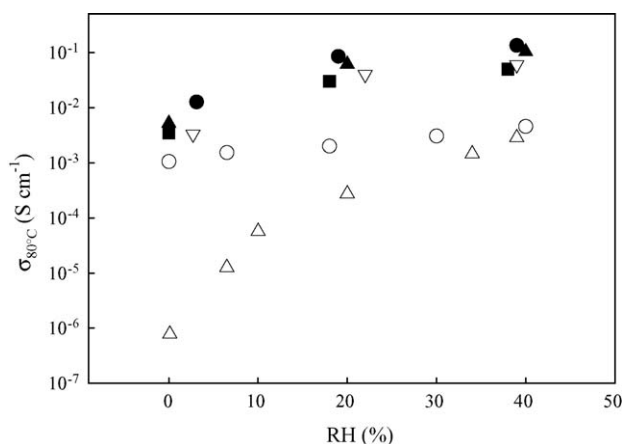


Fig. 4. Proton conductivity vs. relative humidity at 80 °C for all the investigated membranes. ABPBI, $N' = 1.1$ (open circles); PBI₄N, $N' = 4.5$ (open triangle down); PBI₄N_a, $N' = 6.1$ (filled squares); PBI₄N_b, $N' = 10.4$ (filled triangles); PBI₅N, $N' = 12.0$ (filled circles). The conductivity values of NafionTM 117 are plotted as comparison (open triangle up).

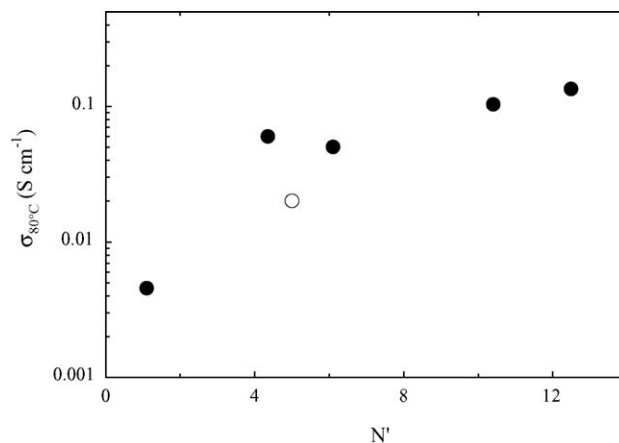


Fig. 5. Membrane proton conductivity as a function of the acid doping level, N' , at 80 °C and RH = 40%. The value obtained by Li et al. [9] for a commercial PBI membrane (open circle), in the same experimental conditions, is reported as comparison.

PBI-based membranes are not greatly affected by the hydration level, mostly for relative humidity higher than 20%. All the films show high proton conductivity even without humidification and values higher than 0.1 S cm⁻¹ at RH = 40% are detected in the case of PBI₄N_b and PBI₅N. Particularly encouraging is the region of low moisture level, where the conductivities of PBI-based membranes remarkably exceed those ones of Nafion.

The effect of the monomer structure on the transport properties is better evidenced in Fig. 5, which reports the membrane proton conductivity at 80 °C and 40% of RH, versus the acid doping level (see Table 1). Two main points can be stressed: (i) both the increase of the monomer molecular weight and basicity lead to the increase of the acid uptake and, consequently, of the proton conductivity; (ii) the same effect seems to take place by increasing the N-group interspacing in the polymer backbone. Fig. 5 also shows the value reported by Li et al. [9] for commercial PBI.

Fig. 6 finally reports the conductivity behaviour as a function of the temperature at RH = 40% for the sample PBI₄N_b.

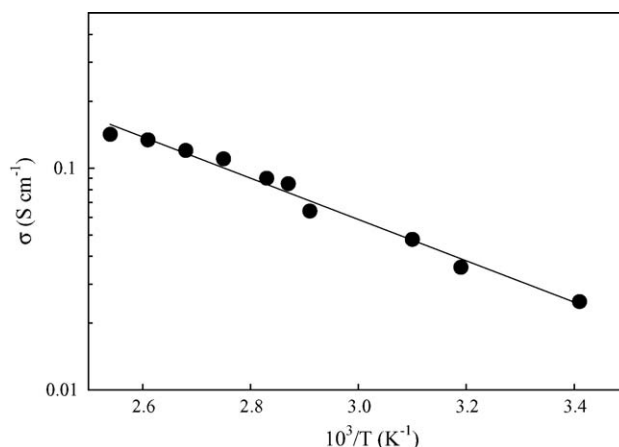


Fig. 6. Plot of the proton conductivity as a function of temperature, at 40% RH, for the PBI₄N_b membrane ($N' = 10.4$).

The logarithm of the conductivity decreases linearly with $1/T$, following an Arrhenius-type behaviour. The activation energy, determined in the range 20–130 °C, is 18 kJ mol⁻¹, which is in good agreement with those generally obtained for the PBI-systems [10]. In particular, energies ranging between 40 and 20 kJ mol⁻¹ were calculated depending on the acid doping level [10,31]. It was seen, that the increase of the doping leads to activation energies approaching that of pure H₃PO₄ system ($E_a = 14.29$ kJ mol⁻¹) [10].

4. Concluding remarks

New phosphoric acid-doped membranes for PEMFCs, based on different polybenzimidazole structures were synthesized, starting from BI-based monomers with increased basicity and molecular weight. They were characterized from a thermal, structural and electric point of view and the results were compared to those of the well-known systems based on ABPBI and commercial PBI.

Each doped film is reasonably stable in the working range of temperature. The membranes show high proton conductivity even in absence of humidification, and values exceeding those of Nafion of three to four orders-of-magnitude were found at low moisture levels. A proton conductivity higher than 0.1 S cm⁻¹ was reached at 80 °C and RH > 30% in the case of the pyridine-based system.

The introduction of extra N atoms in the PBI backbone, as well as their interspacing, remarkably affect the acid doping level and consequently the membrane proton conductivity. The control of these parameters may be therefore a promising way for a further optimization of PBI-based membranes for the fuel cells.

Acknowledgement

This work was financially supported by MIUR (FISR 2001) under the NUME project “Sviluppo di membrane protoniche composite e di configurazioni elettroniche innovative per celle a combustibile con elettrolita polimerico”.

References

- [1] C. Wieser, Fuel Cells 4 (2004) 245.
- [2] G. Alberti, M. Casciola, Annu. Rev. Mater. Res. 33 (2003) 129.
- [3] G. Alberti, M. Casciola, M. Pica, T. Tarpanelli, M. Sganappa, Fuel Cells 5 (2005) 366.
- [4] Q. Li, R. He, J.O. Jensen, N.J. Bjerrum, Chem. Mater. 15 (2003) 4896, and references cited therein.
- [5] K.D. Kreuer, S.J. Paddison, E. Spohr, M. Schuster, Chem. Rev. 104 (2004) 4637, and references cited therein.
- [6] Savadogo, J. Power Sources 127 (2004) 135, and references cited therein.
- [7] J.A. Kerres, J. Membr. Sci. 185 (2001) 3.
- [8] J.S. Wainright, J.-T. Wang, D. Weng, R.F. Savinell, M. Litt, J. Electrochem. Soc. 142 (1995) L121.
- [9] Q. Li, R. He, J.O. Jensen, N.J. Bjerrum, Fuel Cells 4 (2004) 147.
- [10] Y.-L. Ma, J. S. Wainright, M.H. Litt, R.F. Savinell, J. Electrochem. Soc. 151 (2004) A8.
- [11] C.E. Hughes, S. Haufe, B. Angerstein, R. Kalim, U. Mahr, A. Reiche, M. Baldus, J. Phys. Chem. 108 (2004) 13626.
- [12] S.R. Samms, S. Wasmus, R.F. Savinell, J. Electrochem. Soc. 143 (1996) 1225.
- [13] J.J. Fontanella, M.C. Wintersgill, J.S. Wainright, R.F. Savinell, M. Litt, Electrochim. Acta 43 (1998) 1289.
- [14] R. Bouchet, S. Miller, M. Duclot, J.L. Souchet, Solid State Ionics 145 (2001) 69.
- [15] J.-T. Wang, R.F. Savinell, J. Wainright, M. Litt, H. Yu, Electrochim. Acta 41 (1996) 193.
- [16] Q. Li, R. He, J.-A. Gao, J.O. Jensen, N.J. Bjerrum, J. Electrochem. Soc. 150 (2003) A1599.
- [17] I.M. Petrushina, V.A. Bandur, F. Cappeln, N.J. Bjerrum, R.Z. Sorensen, R.H. Refshauge, Q. Li, J. Electrochem. Soc. 150 (2003) D87.
- [18] Z.L.J.S. Wainright, R.F. Savinell, Chem. Eng. Sci. 59 (2004) 4833.
- [19] J.D. Holladay, J. S. Wainright, E.O. Jones, S.R. Gano, J. Power Sources 130 (2004) 111.
- [20] Celanese brochure on www.celanese-ventures.com.
- [21] M.Y. Jang, Y. Yamazaki, J. Power Sources 139 (2005) 2.
- [22] P. Staiti, M. Minutoli, S. Hocevar, J. Power Sources 90 (2000) 231.
- [23] P. Staiti, M. Minutoli, J. Power Sources 94 (2001) 9.
- [24] J.A. Asensio, S. Borros, P. Gomez-Romero, Electrochem. Commun. 5 (2003) 967.
- [25] M.J. Ariza, D.J. Jones, J. Roziere, Desalination 147 (2002) 183.
- [26] X. Glipa, M. El haddad, D.J. Jones, J. Roziere, Solid State Ionics 97 (1997) 323.
- [27] D. Mecerreyes, H. Grande, O. Miguel, E. Ochoteco, R. Marcilla, I. Cantero, Chem. Mater. 16 (2004) 604.
- [28] L. Xiao, H. Zhang, E. Scanlon, L.S. Ramanathan, W.-W. Choe, D. Rogers, T. Apple, B.C. Benicewicz, Chem. Mater. 17 (2005).
- [29] J.A. Asensio, P. Gomez-Romero, Fuel Cells 5 (2005) 1.
- [30] M.K. Daletou, N. Gourdoupi, J.K. Kallistis, J. Membr. Sci. 252 (2005) 115.
- [31] L. Xiao, H. Zhang, T. Jana, E. Scanlon, R. Chen, E.-W. Choe, L.S. Ramanathan, S. Yu, B.C. Benicewicz, Fuel Cells 5 (2005) 287.
- [32] A. Asensio, S. Borros, P. Gomez-Romero, J. Polym. Sci., Part A: Polym. Chem. 41 (2002) 3703.
- [33] S. Jenkins, K.J. Jacob, M.B. Polk, S. Kumar, T.D. Dang, F.E. Arnold, Macromolecules 33 (2000) 8731.
- [34] A. Wereta, M.T. Gehatia, Polym. Eng. Sci. 18 (1978) 204.
- [35] J. Cho, J. Blackwell, S. Chvalun, M. Litt, Y. Wang, J. Polym. Sci.: Polym. Phys. 42 (2004) 2576.
- [36] H. Pu, Q. Liu, Polym. Int. 53 (2004) 1512.